Molecular Crystals and Liquid Crystals
Publication details, including instructions for authors and subscription information:
http://www.tandfonline.com/loi/gmcl16

Far Infrared Study of Solid Cyclohexanol

E. Ściesińska [a] & J. Ściesiński [b]

[a] Institute of Physics of the Jagiellonian University, Cracow, Poland

[b] Institute of Nuclear Physics, Cracow, Poland

Version of record first published: 28 Mar 2007.

To cite this article: E. Ściesińska & J. Ściesiński (1979): Far Infrared Study of Solid Cyclohexanol, Molecular Crystals and Liquid Crystals, 51:1-2, 9-27

To link to this article: http://dx.doi.org/10.1080/00268947908084689

Mol. Cryst. Liq. Cryst., 1979, Vol. 51, pp. 9–28

Printed in Holland

Far Infrared Study of Solid Cyclohexanol†

E. ŚCIESIŃSKA

Institute of Physics of the Jagiellonian University, Cracow, Poland

and

J. ŚCIESIŃSKI

Institute of Nuclear Physics, Cracow, Poland

(*Received January 5, 1978; in final form July 5, 1978*)

The temperature dependence of FIR absorption spectra of cyclohexanol $C_6H_{11}OH$ has been measured in the 35–500 cm^{-1} frequency range and 93–303 K temperature range. All known solid phases were identified. In addition, one metastable phase MS was found.

All phases reveal both equatorial and axial conformers and intermolecular hydrogen bonding. The differences stem from the various types of the bond, viz., chain polymers for phases III and MS and cyclic dimers for phase II, and the cis-, trans- or gauche position of the OH group. The most probable space groups are given.

INTRODUCTION

Cyclohexanol (CHOL) is an especially interesting molecular crystal because it is a plastic crystal[1] and, at the same time, a hydrogen bonded crystal. An excellent review of earlier studies concerning it is given by de Mul.[2] The plastic properties of the high-temperature solid phase I were established by White and Morgan[3] by the dielectric method. The latest and most complete calorimetric study was made by Adachi *et al.*[4] In addition, they found two low-temperature solid phases III and II with transition points at 244.8 K and 265.3 K, respectively. There is some inconsistency in the various papers regarding the notation of these phases. We have followed Adachi's work.

---

† Preliminary results of this work are contained in the Proceedings of the XIII European Congress on Molecular Spectroscopy, Wrocław, Poland, 1977. Subsequent experiments rendered some changes necessary.

They also carefully examined the properties of supercooled crystal I and named it a glassy crystal. Nevertheless, the phase situation in solid CHOL still remains unclear. The number of ascertained solid phases varies from four to seven, depending on the method and the author.[3–5]

The Raman effect and absorption in the mid infrared region for liquid and plastic phases were investigated by several authors.[6–8] There are also some data on other phases[4,8] and infrared spectra[4] up to 200 cm^{-1}. A relatively extensive Raman study on polymorphism in cyclohexanol has been published recently.[9] The authors give a more or less complete assignment of the internal modes of the molecule based on the comparison with cyclohexane.

There are several papers on the crystal structure as examined by the X-ray diffraction method.[10] Phase I was found to be f.c.c. with four molecules per unit cell, and some statical or dynamical orientational randomness of molecules is suggested. There is no reliable data available on low-temperature phases, only some remarks that they should be less symmetrical, perhaps monoclinic as in cyclohexane.

The aim of this work was to obtain as much information as possible about the properties, differences and similarities of low-temperature phases. It is our belief that the investigated spectral region is the most suitable for this purpose because it is associated with the lattice and low energy skeletal modes of the molecule.

EXPERIMENTAL PROCEDURE AND RESULTS

Absorption measurements were carried out with two Fourier transform spectrometers with a Michelson interferometer: a slow scanning Grubb Parsons IRIS in the 80–480 cm^{-1} region and a fast scanning DIGILAB in the 35–500 cm^{-1} region. Polyethylene windows were used as the sample holder. Sample temperature was stabilized and measured with a copper-constantan thermocouple to an accuracy of ±0.5 K, but the systematical error can be somewhat higher. Resolution was 0.5, 2, 4 or 8 cm^{-1} for the various runs. Commercial cyclohexanol, fractionally distilled and checked for purity by gas chromatography, was used. The sample holder was filled with a liquid CHOL layer 0.1 or 0.2 mm thick and several runs of the temperature dependence of absorption spectra were made under various cooling and heating conditions. Some representative results are shown in the figures. All spectra except that in Figure 1 were recorded on a DIGILAB.

In Figure 1 is presented the IRIS run made according to the diagram in Figure 2, which gives the temperature dependence of integral transmission. Integral transmission is defined as transmitted power in the whole frequency range. This kind of diagram exposes phase transitions distinctly, as they most

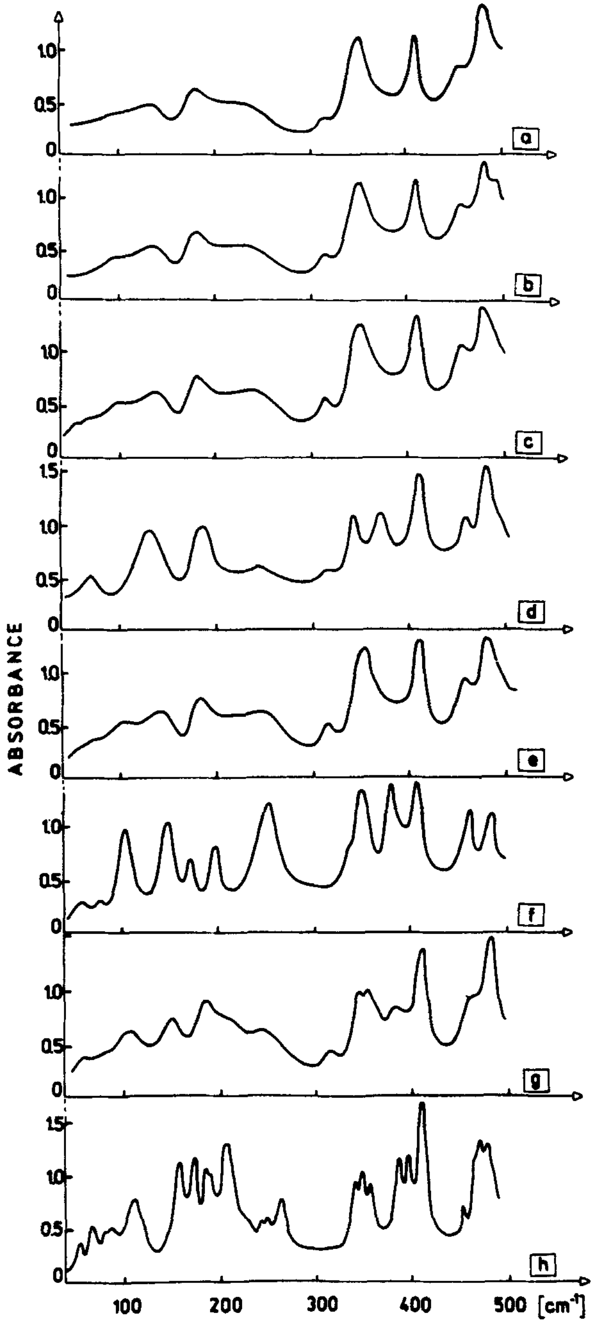

FIGURE 1 The CHOL absorption spectra for various temperatures: representative run for IRIS spectrometer. Resolution 8 cm^{-1} for a–e and 4 cm^{-1} for f–h spectra. Temperatures: 288, 253, 224, 202 and 87 K for spectra b, c, e, g and h (cooling) and 227, 254 and 303 K for f, d and a (heating), respectively. Phases: a liquid, b supercooled liquid, c and e plastic, d crystal II, f crystal III, h crystal MS.

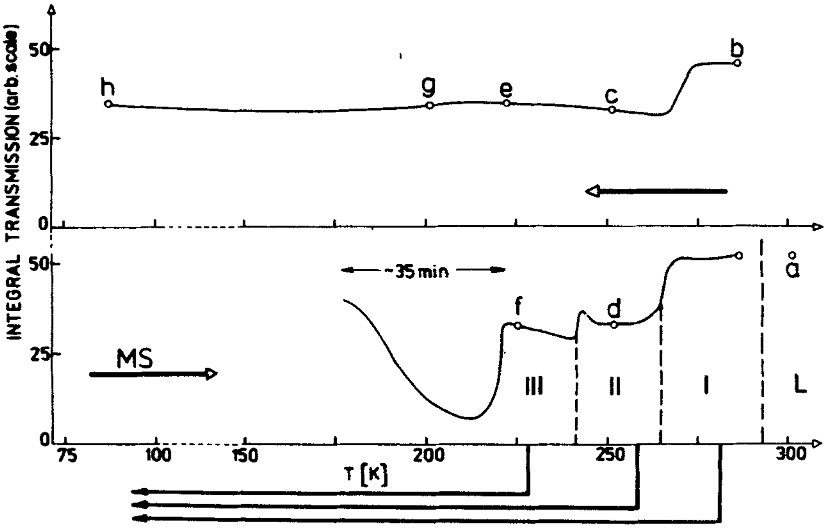

FIGURE 2 The integral transmission diagram for the run in Figure 1 : letters a–h and points denote absorption measurements in accordance with Figure 1.

frequently cause a change of integral transmission due to increased scattering even in cases when the absorption is similar for both phases. The various phases were grown also according to this diagram. Slow heating from liquid nitrogen temperature always gives phase III above ca 220 K which transforms to phase II at ca 245 K. Adachi[4] and other authors take this transition to be the phase III–phase I transition. But at the same time Adachi has admitted that there is some trouble with phase I stability below 265 K and with the sluggish irreversible transition to phase II. Our results show no doubt in this respect, a relatively abrupt and fast III–II transition always takes place at ca 245 K. It can also appear a few degrees lower, but then it is much slower; an example at 238 K is shown in Figure 3. Both crystals III and II are stable between 90 K and their transition points; Figure 4 shows spectra for the various temperatures for crystal II.

Special requirements must be fulfilled in order to grow the metastable phase denoted MS which had not been observed up till now. Figure 5 shows an example of its growth at 203 K. Phase MS is usually contaminated by phase III; this is seen from the trace amount of the 262 cm^{-1} mode, which is characteristic only for crystal III (Figure 1, h and f, and Figures 3, 5 and 6). Its relative intensity strongly changes from run to run, but we have failed to achieve a pure MS phase. Upon slow heating the MS crystal transforms to crystal III in the ca 175–220 K range (Figure 1, h and f, and Figure 2). But fast heating undoubtedly gives a direct MS–I transition between 238 and 250 K; we did

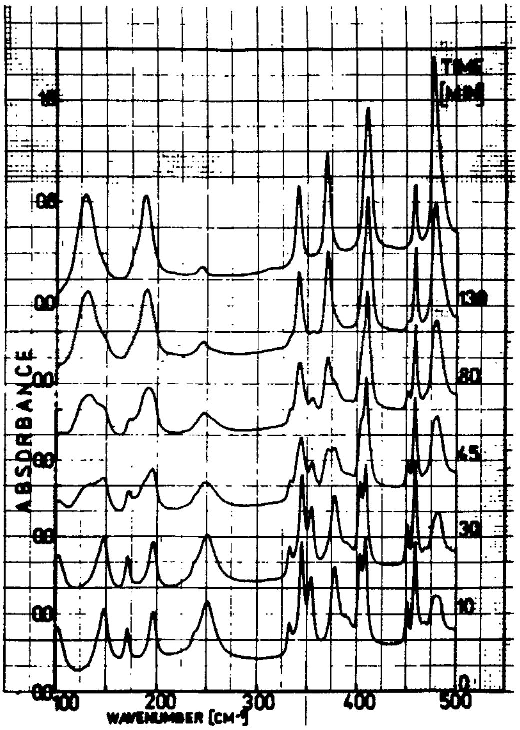

FIGURE 3 Spectrum variations during phase III to phase II transition at 238 K. Resolution 2 cm^{-1}. Time delay 0, 10, 30, 45, 80 and 130 min.

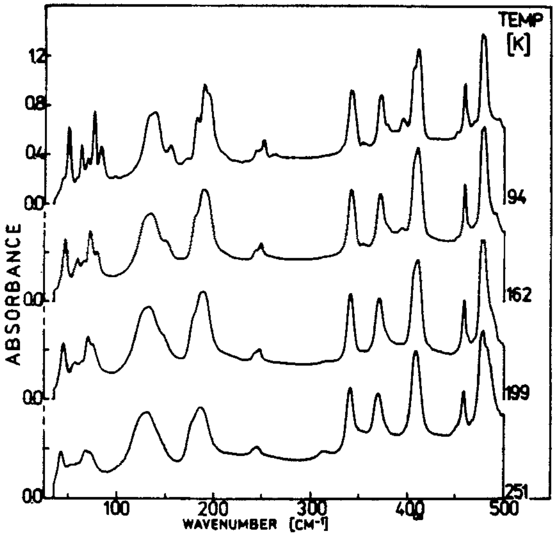

FIGURE 4 Temperature dependence of phase II spectra. Resolution 2 cm^{-1}.

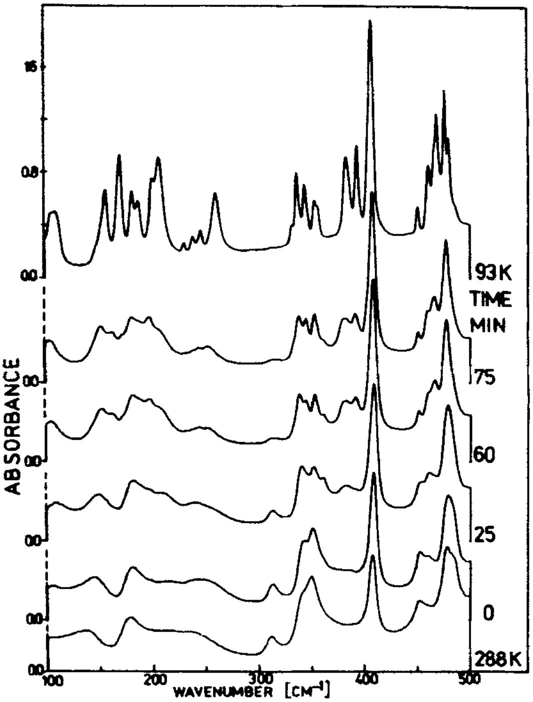

FIGURE 5 Time development of MS phase from supercooled phase I at 203 K. Time delay 0, 25, 60 and 75 min.

not define the transition point more precisely. The temperature range of some instabilities and strange behaviours has also been observed by several other authors.[4,5] All additional phases—pre-II of Green, II′ and III′ of Adachi[5]—are associated with this range. It now seems possible that they were not pure phases but mixtures.

The results for different phases and temperatures are gathered in Tables I and II.

DISCUSSION

1 Molecular conformations

The cyclohexanol molecule $C_6H_{11}OH$ can have several conformations depending on whether the cyclohexane ring conformation is of the chair, boat or skew boat form and whether the OH group position is equatorial or axial. The chair form is known to have a much lower energy than the boat one. The energy difference amounts to 5.5 kcal/mol for cyclohexane,[11] and even for

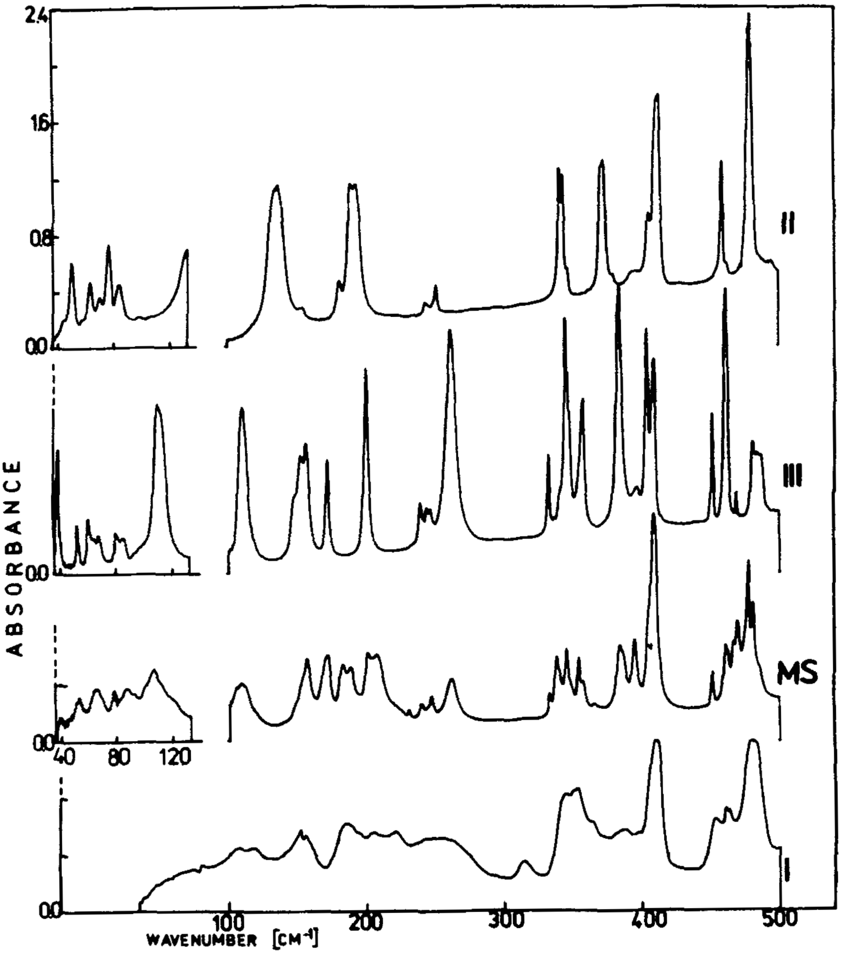

FIGURE 6 Solid phases at 93 K. Resolution 0.5 cm^{-1} for phases II, III and MS and 2 cm^{-1} for supercooled phase I and low energy part of phase II.

six-membered heterocyclic aliphatic ring compounds it is similar.[12] Hence, for the liquid and solid states the boat form can be unquestionably disregarded.[13,14]

The energy difference between the axial and equatorial conformations is, generally speaking, much lower. The spectroscopical methods give 0.4–0.8 kcal/mol for CHOL.[6,8,9] This gives a significant amount of the axial form in the liquid near the melting point. For solids, for the pure phase at least, it is usually assumed that only one lower-energy form remains.[13] This, however, is not necessarily the rule. The authors of References 4, 6, 8 and 9 find a CO

TABLE I

Internal mode frequencies (cm^{-1}) and assignment

Crystal MS		Crystal III			Crystal II		Crystal I	Liquid
Molecular Symmetry Species		Molecular Point Group C_1						
	93 K	93 K	148 K	240 K	94 K	253 K	288 K	303 K
	231 w							
A'	240 w	240 w	240	trace	243 w	245		
A''	247 w	245 w 247 w	245	trace	251 m			
?							312 m	312 m
A'	332 w	332 m	332	333	341 s			
	337 m	336 w						
	339 sh							
		340 sh						
A'	345 w	345 vs	345	345	343 s	340	350 s	347 s
	349 sh	347 sh						
	353 m							
A''	*356 sh	357 s	356	355	346 m			
	*383 sh							
$A'a$	385 m	383 vs	382	379				
	394 s	396 m	394	390	372 s	370		
					379 wsh			
					*395 wb			
		404 vs	404	404	*405 m			
$A''e$	409 vs	409 vs	409	410	411 vs	411	408 s	407 s
	451 w	451 m	452	452	459 s	458	453 m	453 m
$A''a$	*460	461 vs	460	460				
		468 vw	468	trace				
	466 sh							
$A'e$	468 s	480 m	484	484	478 vs	479	480 vs	480 vs
	476 vs	485 m						
	480 s							

Notation: s = strong, m = medium, w = weak, v = very, b = broad, sh = shoulder, *e* = equatorial and *a* = axial conformation; asterisks mark spurious bands from phase III admixture.

TABLE II

Lattice mode frequencies (cm^{-1})

	Hydrogen-bonded chain polymers						Hydrogen-bonded cyclic dimers		
			Crystal III				Crystal II		
Assignment	Crystal I 288 K	Crystal MS 93K	93 K	148 K	203 K	240 K	94 K	162 K	251 K
		39 w	39 m				44 sh		
							49 s	47	43
		52 w	53 w	51	48				
							57 w		
			61	60	58	55			
		65 m	65 m				62 m	59	52
oph			68	67	65	64			
							69 w		
		77 w	81 w						
		86 m	86 w	82	80	76	76 s	73	68
		92 sh							
							83 m	80	73
	95	105 s	110 s	109	106	102			
							97 vw		
iph									
	135		151 sh						
			153 s						
		157 s	157 s	155	151	148	136 vs	134	130
							D 153 m	151	
		171 s	173 s	173	173	171			
	180	182 s					181 m		
		188 s					D 190 vs	189	187
hs							193 sh		
		*201	201 vs	200	199	196			
		206 vs							
	235								
		*261	262 vs	258	255	251			

Additional notation in comparison with Table I: oph and iph for hydrogen bond out-of-plane and in-plane bending modes and hs for hydrogen bond stretching mode ν_{σ}; D = dimer internal mode.

stretching band for both conformations in CHOL's plastic phase, while Adachi[4] also found both even in crystal III. The conversion between the axial and equatorial forms has to go through a chair-boat, chair-skew boat or chair-chair interconversion, so that the activation energy must be large, about 10 kcal/mol.[11]

There should also be taken into account the possibility of the OH group occupying a cis, trans or gauche position relative to the nearest proton, but no adequate data are available in this respect.

2 Internal modes

The best way of carrying out the assignment for CHOL is by comparing it with cyclohexane, because one should expect strong similarity between these molecules, since the cyclohexane spectrum of all the phases is among the best recognized ones.[15,16] Figure 7 gives the correlation diagram between the D_{3d} point group of cyclohexane and the C_s point group of CHOL molecules.

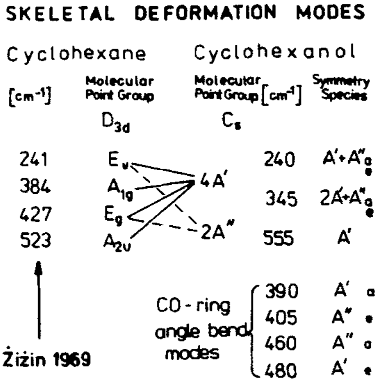

FIGURE 7 Correlation diagram for the D_{3d} and C_s molecular point groups of cyclohexane and CHOL; *e* is equatorial and *a* is axial conformation.

The point group analysis gives for twelve cyclohexane skeletal modes the irreducible representation $\Gamma^c = 2A_{1g} + 2E_g + 1A_{1u} + 1A_{2u} + 2E_u$. After subtraction of six CC stretching modes there remains, for the six low-energy ring deformation modes, the irreducible representation $\Gamma_s^c = 1A_{1g} + 1E_g + 1A_{2u} + 1E_u$. In addition, the CHOL molecule has one heavy oxygen atom outside the ring, so one out-of-plane A'' and one in-plane A' angle bending mode should be added. Hence, the irreducible representation Γ^0 of eight low-energy deformation modes of CHOL is $\Gamma^0 = 5A' + 3A''$.

Figure 7 also gives the tentative band assignment for CHOL. The cited frequencies are mean values for the whole band at the lowest temperature. This assignment was based on the following: compatibility of the assignment of all phases; C_s is the effective symmetry of the molecule at least for the MS phase because for C_1 the different multiplicities (singlets and doublets) of internal modes could not be explained; the 240 cm^{-1} mode is almost constant even for heterocyclic six-membered ring compounds;[12] ring deformation modes should not depend much on conformation, whence they can be assumed to be equal for both isomers, in contrast to CO-ring angle bending modes; the depolarization ratio for higher modes;[7,9] bands weak for liquid and stronger for solids belong to the axial form; and the splittings especially strong for CO modes are correlation splittings.

The 312 cm^{-1} band (Table I) needs separate discussion. This band appears for liquid and plastic phases with similar intensity, but disappears for properly grown ordered phases (Figure 1 and Figures 3 to 6). At first it was supposed to be the OH torsion mode of monomers and terminal groups of polymers. This band can be expected below ca 400 cm^{-1} for alcohols;[17] for methanol[18] it was observed at ca 250 cm^{-1}. This suggestion was canceled by measurement on deuterated sample $C_6H_{11}OD$ which reveals a similar band at the same place (complete results will be published separately). The other possibility is that this is a difference band of internal modes, namely the 555–240 cm^{-1} mode. But temperature dependence does not support this assignment distinctly: mode intensity seems to be dependent only on the degree of order of the crystal as it changes at a stable temperature in the course of growing an ordered phase (Figure 5). The most probable is to assign the 312 cm^{-1} band to an internal mode of an unbonded molecule which is strongly affected by hydrogen bonding. A careful examination of several runs of growing all ordered phases (e.g. Figure 5) shows that the 390 cm^{-1} band rises simultaneously with the diminishing of the 312 cm^{-1} band. Therefore, it is believed that the 312 cm^{-1} band is the A' CO-ring angle bending mode of axial conformer for unbonded molecule which shifts ca 80 cm^{-1} under formation of the hydrogen bond. This also means that a significant percentage of the axial molecules does not participate in hydrogen bonding for disordered phases. The basis for supporting that such a shift is possible stems from the study of phenol-pyridine complexes[19] which seems to be the most closely related case available in the literature. These complexes show a much weaker hydrogen bond as the ν_σ mode is in the range of 100–130 cm^{-1} compared to 200–260 cm^{-1} for CHOL (see Table II). Nevertheless, an experimental shift for a similar mode of phenol reaches 32 cm^{-1}.

Complete results and final tentative assignments for internal modes are given in Table I.

3 Phase I

The frequency range of the CHOL spectra presented in this paper can be divided roughly into two parts, viz., the range of lattice modes, below ca 280 cm^{-1}, and that of internal modes over this value. The first part does not reveal any difference between the liquid and plastic phases (Figure 1, a or b and c); this is a characteristic feature of all plastic crystals.[20] On the other hand, the spectrum from plastic crystals without the hydrogen bond is quite different and always shows one broad band. The structure observed for CHOL is associated with the hydrogen bond bending and stretching modes.[21,22] It is seen that hydrogen bond properties do not change markedly upon freezing. Under further cooling the spectrum changes more or less, depending on the cooling rate. Faster cooling gives a glassy crystal with no significant change up to 90 K. Slower cooling usually produces a mixture of solid phases. This shows up in the structure of the broad band (Figure 6, I the glassy crystal with some admixture).

The internal mode range, from the liquid to glassy crystal at 90 K, also shows no significant differences—only the CO band of the axial form at 390 cm^{-1}, shuttered by neighboring bands completely for the liquid, appears at lower temperatures.

Qualitative assignments of the hydrogen bond modes, based on comparison with literature data for other substances, are given in Table II.

4 Low-temperature phases

The most important in the subsequent discussion of results are CO modes, specifically, their behavior in crystals (Table I). Both A' and A'' are doublets for crystal III and singlets for crystal II and only A' remains a doublet for crystal MS. These splittings are much more pronounced than for other internal modes. They are obviously caused by the hydrogen bond between identical isomers, as this intermolecular interaction should be the strongest one and should mainly influence the CO modes. It is known that chain associates are formed in liquid CHOL.[23] For solid alcohols not much data are available; hydrogen bonded chains were ascertained for methanol[22,24] and *n*-hexadecanol.[25] The methanol chain probably has C_2 or C_{2v} line group symmetry.[22,24] The same groups could be expected for cyclohexanol. The third one involving the symmetrical hydrogen bond, C_{2h}, is excluded because the OH stretching band[4] points to a weak bond.[26]

4.1 *MS phase* The CO modes point to the existence of both isomers and the C_s point group symmetry of the molecule in this phase. Therefore, the

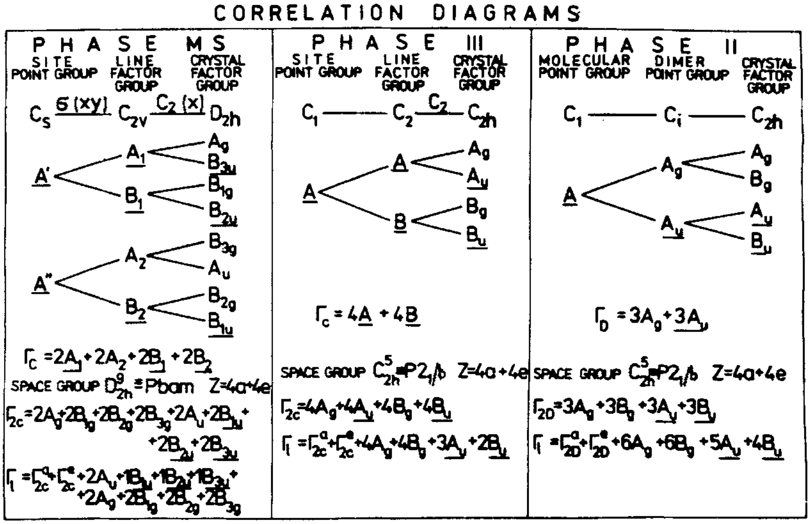

FIGURE 8 Correlation diagrams for phases MS, III and II of CHOL. IR active species underlined. Γ_l, Γ_c, Γ_{2c}, Γ_D and Γ_{2D} denote the factor group irreducible representations of the lattice modes, intrachain modes, intrachain modes of the two coupled chain units per crystal unit cell, intradimer modes and intradimer modes of the two coupled dimers per crystal unit cell, respectively. Z denotes the number of molecules per crystal unit cell.

C_{2v} line group is the only possible chain symmetry. The primitive unit cell should contain at least four molecules ($2a + 2e$) as twelve unquestionable lattice modes are observed (Table II). The correlation method[27] enables the performance of a factor group analysis similarly as was done by Durig[24] in the case of methanol. The correlation diagram (Figure 8) gives the results. It is seen that intrachain interactions should give an infrared active doublet for all internal A' modes and a singlet for all A'' modes.

Further knowledge about chain geometry can be acquired by studying the relative intensities within the CO doublets. According to the oriented gas model[28,29] the intensity ratio $I|A_1| \,\|\, I|B_1|$ of the A' doublet for the C_{2v} chain equals $\cot^2 \theta$, where θ denotes the angle between the chain axis and A' transition moment direction. The lower energy component should be A_1 under the assumption that dipole–dipole coupling of transition moments is the predominant intermolecular interaction.[30] Such an assumption is quite reasonable for CO modes. An experimental value of the θ angle for both equatorial and axial chains was found to be 54 ± 4 deg. Knowledge of the θ angle and conventional intramolecular parameters[4,31] allowed the graphical construction of molecular chains shown in Figure 9 to be made. The direction of the A' transition moment of the CO mode was taken to be perpendicular to

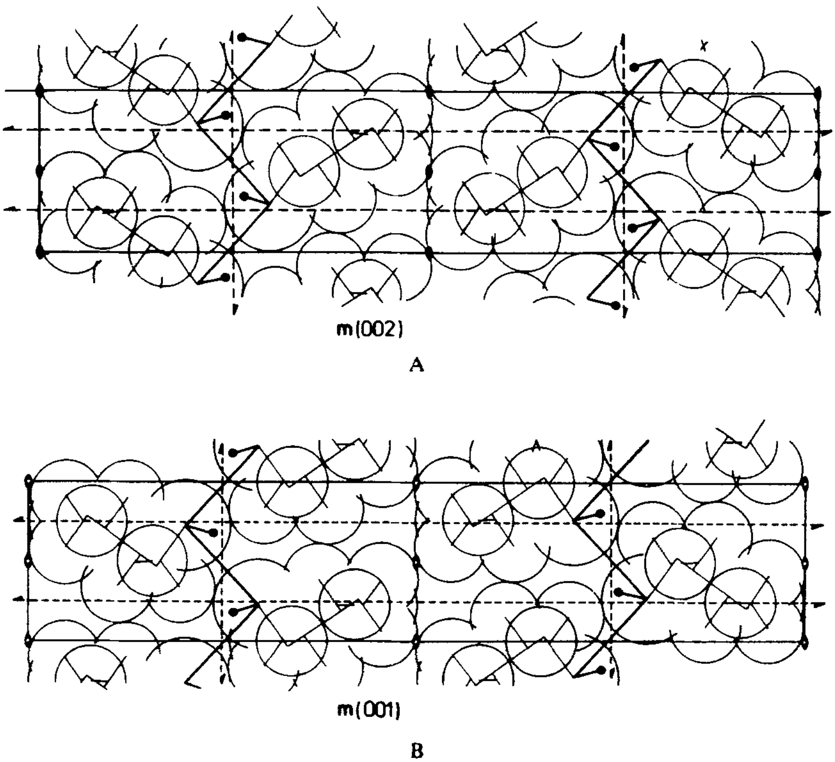

FIGURE 9 Unit cell of MS phase for the D_{2h}^9 space group. A—the layer of equatorial molecule chains, B—the layer of axial molecule chains.

the CO bond, oxygen and hydrogen atom radii and OH bond length equal to 1.52, 1.17 and 0.96 Å, respectively.

According to Kitaigorodski[31] the rule of compact packing is the most important rule for molecular crystals, and any specific directional interactions such as hydrogen bonding[32] cannot change the optimal crystal structure by more than a few per cent. Two space groups, namely, $C_{2v}^2 = Pmc2_1$ and $D_{2h}^9 = Pbam$ from the orthorhombic system fulfil this rule equally well in the case of the MS phase. Both give a sandwich-like crystal structure, i.e. the crystal consists of layers of equatorial and axial chains in turns. The two-dimensional space group of each layer is *pgg* for the second case. This group ensures fulfillment of Kitaigorodski's rule for any orientation of a plane figure with the inversion center within the unit cell with properly chosen lattice constants. The equatorial and axial layers for the *Pbam* space group are shown in Figures 9A and 9B, respectively. It is seen that equatorial planes of molecules are parallel in both layers—this enables compact packing between the layers, too. The crystal unit cell contains two equatorial and two axial chain units, i.e. $Z = 8$ ($4e + 4a$). At the same time, Figure 9 shows the unit cell for the $Pmc2_1$ space group when a solitary chain unit is considered. This will cause the inversion centers and the two-fold $2(z)$ and $2_1(y)$ axes to disappear.

The correlation diagram (Figure 8) gives the number and symmetry species of the lattice modes for the *Pbam* space group. There should be fifteen infrared-active lattice modes. Of these, three interchain translations should have low energy and may be beyond the experimental range. Comparison with the twelve observed modes shows the agreement to be quite good. A similar situation is for the $Pmc2_1$ space group ($Z = 2a + 2e$); there should be twelve intrachain and three interchain infrared-active lattice modes. We have chosen the *Pbam* group for two reasons. The first is the compensation of static dipole moments. This may also be achieved for the $Pmc2_1$ group, but this is not due to symmetry. The second reason is that under high resolution conditions a trace of crystal correlation splitting was observed for the symmetrical CO mode of equatorial form (Figure 6 and Table I). Two gerade components are infrared inactive and cannot be observed for ordered crystals. But it is seen from the spectra, particularly from the lattice mode range, that the MS phase is a disordered phase because all of the lattice modes are rather broad. Disorder may be due to a phase III admixture, but it seems rather to be an intrinsic property of the MS phase. This follows from the fact that the broadness does not depend much on the amount of phase III; the experimental spectra seem to be a simple aggregate of pure phase spectra in proper proportions. In our opinion, this disorder presumably stems from the gauche positions of the OH groups for equatorial chains. It is very likely that *e* and *a* isomers have different stable positions, although there is no reliable data which would confirm this. Our results agree with the cis position for both conformers, but this may only be a statistical order involving two different gauche positions in a real crystal.

Table III gives estimated values of some more crystal parameters. The packing parameter and density values are quite reasonable.[31,33] The hydrogen bond parameters, particularly its length, are near the acceptable limit.[26,32] Nevertheless, too much attention should not be given to the numerical figures themselves, because actual intramolecular parameters, especially bond angles[34] and the transition moment direction, can be somewhat different.

The lattice mode assignments could not be made on the basis of experimental data, and only a qualitative classification into hydrogen bond stretching and bending modes is given in Table II. Since the site point group does not contain an inversion center, translational and librational modes are mixed.

TABLE III

Predicted structures

Phase	CO modes		Site point group	Chain line group	2-dim layer group	Crystal space group	Z	Lattice modes		OH position		Lattice parameters
	A'	A''						Np	Ne	a	e	
MS	d	s	C_s	C_{2v}	pgg	D_{2h}^9	$4a$ + $4e$	15	12	cis	cis	a = 5.4 K = 0.66 b = 26 c = 9.5 l = 3.6 ρ = 1.0 β = 32°
III	d	d	C_1	C_2	pgg	C_{2h}^5	$4a$ + $4e$	21	14	g	g	—
				Dimer point group								
II	s	s	C_1	C_i	pgg	C_{2h}^5	$4a$ + $4e$	21	13	g	g	—

Notation: s = singlet, d = doublet, g = gauche, Np and Ne—predicted and experimental number of ir active lattice modes; a, b and c—lattice constants and l—hydrogen bond length, in Å; β—hydrogen bond angle; K—packing parameter; ρ—density, in g/cm^3.

4.2. *Phase III* Phase III is surely an ordered phase; some lattice modes have a half width of only 3 cm^{-1}. The CO doublets reveal that molecules lost their symmetry plane and that both conformers are present. In accordance with the discussion above, we chose the C_{2h}^5 space group as the most probable one. Some other data are given in Table III. The correlation method predicts twenty one infrared active lattice modes (Figure 8). Of these, three interchain translations and two chain rotations can be expected to have very low energy. This is in good agreement with the fourteen experimental modes. It is very likely that all differences between the MS and III phases follow from the gauche position of the OH groups in both conformers. This has to cause some revolving of molecules, which shows up as reversed relative intensity within the line correlation doublets of internal modes.

4.3 *Phase II* The behavior of the lattice mode range is the most characteristic for phase II and different than that of the other phases. The low energy part containing eight modes is like that of a normal ordered crystal, i.e. the modes are strongly sharpened and shift towards higher energies when cooling is applied (Figure 4). But the high energy part contains only two broad bands with some structure seen at the lower temperatures only. At the same time their energy shift is much less pronounced. All CO modes, on the other hand, become singlets and reveal both conformers. As was stated earlier, only singlets cannot appear in the case of chain structure when the hydrogen bond is a weak one.

All of these unusual properties fit the structure of cyclic dimers very well. The two bands are internal modes of axial and equatorial cyclic dimers. Each dimer should have three infrared active internal modes for a possible C_i or C_{2h} point group symmetry. The likely crystal factor groups would be the C_{2h} or D_{2h} group, respectively. The second one demands seven infrared active external modes of dimers and the C_s molecular point group. When considering the eight low energy modes observed, the D_{2h} group should be rejected. Figure 8 shows the correlation diagram for the C_{2h} crystal factor group. It is seen that there should be nine infrared active external modes of dimers i.e. translations of the dimers and interdimer coupling should split the internal modes of dimers into doublets. This splitting appears as an overall broadening of dimer internal modes in experimental spectra. The C_1 molecular point group reveals that gauche positions of the OH group are involved. The most probable space group seems to be the C_{2h}^5 group, in accordance with Kitaigorodski's rule. Some further information is given in Table III.

5 Comparison with Raman studies

The main topic of the paper by James *et al.*[9] is the plastic phase which we had put aside in our discussion. Their conclusions concerning ordered phases, however, are almost opposite to ours. They measured two ordered phases which they named II and III and concluded that there is no axial conformation for both phases; the hydrogen bond exists only in phase III.

It is known that the hydrogen bond properties are hardly seen in the Raman effect. For example, James *et al.* do not observe any hydrogen bond modes for liquid and plastic phases, which occur in our spectra without any doubt. As regards the axial conformer, it is impossible to give a coherent internal mode assignment for all five phases without both conformers in our case. We have also observed strong intensity changes (3–10 times) between phases for some internal modes particularly the 460 and 480 cm^{-1} bands. But it is known that the hydrogen bond behavior strongly influences transition moments for some modes. It seems that the OH group position should influence transition moments also.

We made an attempt to grow phases according to the method of James *et al.* in order to check the nomenclature. After waiting seven hours at 255 K with no change in the spectrum we had to abort the project. We believe that James' phase III is identical with our phase II.

CONCLUSIONS

Four solid phases were identified: crystal I, II, III and metastable crystal MS. All phases contain both equatorial and axial conformers, and all phases reveal the hydrogen bonding. The most probable space groups for low-temperature phases are given in Table III. The outcome of the competition between the compact packing, the *cis-*, *trans-*, or *gauche* position of OH groups and the strength of the hydrogen bond seems to dictate the structural and dynamical properties of cyclohexanol.

Acknowledgments

We wish to express our gratitude to Professor J. Janik for his kind interest and stimulating discussions. This work was initiated by Mr. J. Lenik in connection with his dielectric research, and we would like to express our appreciation of his helpful advice and discussions and also for making his unpublished results accessible. We thank Mr. J. Sokolowski, W. Olejarczyk, M. Rydzy, W. Słomczyński and Miss E. Link for their help with the measurements.

References

1. J. Timmermans, *J. Phys. Chem. Solids*, **18**, 1 (1961).
2. F. F. M. de Mul, Ph.D. thesis, Technische Hogesschool Delft (1973).
3. A. H. White and S. O. Morgan, *J. Am. Chem. Soc.*, **57**, 2078 (1935).
4. K. Adachi, H. Suga and S. Seki, *Bull. Chem. Soc. Japan*, **41**, 1073 (1968).

5. J. R. Green and W. T. Griffith, *Mol. Cryst. Liq. Cryst.*, **6**, 23 (1969); K. Adachi *et al.*, *Mol. Cryst. Liq. Cryst.*, **18**, 345 (1972); J. R. Green and W. T. Griffith, *J. Cryst. Growth*, **5**, 171 (1969).
6. P. Neelakantan, *Proc. Indian Acad. Sci.*, **A57**, 94 (1963).
7. B. D. Saksena, *Proc. Indian Acad. Sci.*, **A12**, 330 (1940).
8. W. Masschelein, *J. Mol. Spectry.*, **10**, 161 (1961).
9. D. W. James, H. F. Shurvell and R. M. Parry, *J. Raman Spectr.*, **5**, 201 (1976).
10. D. R. Wheeler, Ph.D. thesis, University of New Mexico (1968).
11. C. W. Beckett, K. S. Pitzer, and R. Spitzer, *J. Am. Chem. Soc.*, **69**, 2488 (1947); F. R. Jensen *et al.*, *J. Am. Chem. Soc.*, **84**, 386 (1962).
12. J. J. Sloan and R. Kewley, *Can. J. Chem.*, **47**, 3454 (1969).
13. P. Klaeboe, *Acta Chem. Scand.*, **23**, 2641 (1969).
14. D. W. Scott and G. A. Crowder, *J. Chem. Phys.*, **46**, 1054 (1967).
15. W. N. Rogovoj and G. N. Żiżin, *Fiz. Tverd. Tela*, **17**, 376 (1975).
16. G. N. Żiżin, M. A. Moskaleva, and J. Sterin, *Spektroskopia Tverdogo Tela* (suppl. to *Opt. Spektrosk. SSSR*), 146 (1969).
17. A. V. Stuart and G. B. B. M. Sutherland, *J. Chem. Phys.*, **24**, 559 (1956).
18. A. J. Barnes and H. E. Hallam, *Trans. Faraday Soc.*, **66**, 1920 (1970).
19. D. L. Cummings and J. L. Wood, *J. Mol. Struct.*, **20**, 1 (1974).
20. C. Brot, B. Lassier, G. W. Chantry, and H. A. Gebbie, *Spectrochim. Acta*, **24A**, 295 (1967); R. Haffmans and I. W. Larkin, *J. Chem. Soc. Faraday Trans. II*, **68**, 1729 (1972).
21. W. G. Rothschild, in: *The Hydrogen Bond* (Eds. P. Schuster, G. Zundel and C. Sandorfy), North-Holland Publishing Company, Amsterdam 1976, Vol. II, p. 767.
22. A. B. Demster and G. Zerbi, *J. Chem. Phys.*, **54**, 3600 (1971).
23. J. Liszi and M. Náray, *Acta Chim. Acad. Scien. Hung.*, **81**, 11 (1974).
24. J. R. Durig, C. B. Pate, Y. S. Li, and D. J. Antion, *J. Chem. Phys.*, **54**, 4863 (1971).
25. I. D. Mikhailov, V. A. Savelev, N. D. Sokolov, and N. G. Bokii, *Phys. Stat. Sol. b*, **57**, 719 (1973).
26. A. Novak, *Structure and Bonding*, **18**, 177 (1974).
27. W. G. Fateley, F. R. Dollish, N. T. McDevitt, and F. F. Bentley, *Infrared and Raman Selection Rules for Molecular and Lattice Vibrations: The Correlation Method*, Wiley-Interscience, John Wiley Sons, Inc., New York, 1972.
28. J. W. Rohleder and T. Luty, *Mol. Cryst.*, **5**, 145 (1968).
29. D. F. Hornig and W. E. Osberg, *J. Chem. Phys.*, **23**, 662 (1955).
30. J. A. Ibers, J. Kumamoto, and R. G. Snyder, *J. Chem. Phys.*, **33**, 1164 (1960).
31. A. I. Kitaigorodski, *Molekularnyje Kristaly*, Izd. Nauka, Moscow, 1971.
32. W. A. P. Luck, Ref. 21, p. 527.
33. J. R. Green and C. E. Scheie, *J. Phys. Chem. Solids*, **28**, 383 (1967).
34. N. W. Aleksiejev and A. I. Kitaigorodski, *J. Struct. Chem. USSR*, **4**, 164 (1963).